Supplementary Electronic Materials for original paper submitted for publication in

Physical Chemistry Chemical Physics

A forgotten participant in pore deblocking of zeolites: dicarbonate in the NaMeA zeolites, Me = Na, K, Rb, Cs

Ilya A. Bryukhanov[a,b], Andrey A. Rybakov[c], Alexander V. Larin*[c]

[a]*Institute of Mechanics, Lomonosov Moscow State University, Moscow, 119192 Russia;*
[b]*Mechanical Engineering Research Institute of RAN, Moscow, 119334 Russia;*
[c]*Department of Chemistry, Lomonosov Moscow State University, Leninskie Gory, Moscow*

Ph. 7-495-939-3952, Fax 7-495-932-8846

TOTAL PAGES 9

TABLES 2

FIGURES 2

*) corresponding author: *nasgo@yandex.ru*

Part S1. Entropy contributions along the AIMD trajectory

The vibrational S_{vib} entropy was evaluated as the most important part of the entropy at low loading (one CO_2 and one CO_3^{2-} *per* two large cages). It was calculated in two points (reagents and products) of the reaction (2) and in some selected points (shown by arrows in Fig. 4a) along the reaction path (3) studied with AIMD. The constant number of 16 atoms (two H atoms, nearest 7 surrounding cations plus the reactive species CO_2 and CO_3^{2-} or $C_2O_5^{2-}$) in each point was allowed to move while calculating the frequencies. This set of 16 atoms seems to be involved in the main changes upon reaction (2) in the system. The other atoms were kept fixed. 48 frequencies were calculated in all points but partition functions were calculated over 46 frequencies because at some of the geometries one or two low frequencies were imaginary. They are usually related to the positions of the cations or CO_2. In order to compare the same sets of the frequencies in all points, two frequencies were deleted from all sets (with imaginary frequencies or real frequencies of respective modes):

$$S_{vib} = k \times N_0 \times \ln(\Pi_{i=1}^{46} \exp(-hc\omega_i/2kT)/(1- \exp(-hc\omega_i/kT)) \qquad (S1)$$

where k is Boltzmann constant, N_0 is Avogadro number. The S_{vib} values were obtained at the N points either in the case of CO_3^{2-} (Fig. 4b, c) or $C_2O_5^{2-}$ (Fig. 4d, e) geometries (the 7 points are depicted by arrows in Fig. 4a plus the initial geometry of reaction (2)) and compared relative to the $S_{vib}(1)$ one in the starting point (3) (or the product of the reaction (2)), *i.e.,* $\Delta S_{vib}(j) = S_{vib}(j) - S_{vib}(1), j = 1,\ldots, N$. The differences between $T\Delta S_{vib}(j)$ values along the reaction paths (2) and (3) vary between -0.027 and 0.042 eV, respectively, at T = 300K (Table S1). It cannot have a significant effect on the free Gibbs energy $\Delta G = \Delta H - T\Delta S = \Delta U - T\Delta S$ (at fixed temperature and pressure) relative to the heats of the reactions (2) or (3) with ΔU = +0.17 eV (between the lower and middle insets in Fig. 3) or -0.265 eV (see Table 2), respectively.

Regarding the B3LYP computations for the frequencies and entropy terms, another method was applied. The TS(i) term including vibrational entropy for 17 atoms (one O atom was

allowed to move relative to the set of 16 atoms at the PBE-D3/PAW level) was calculated by the CRYSTAL code (Table S2). The TS(i) were calculated at 298.15K (not 300K), but we neglected the small difference. The TS values vary around the average value of 1.239 eV/cell with the exception of the point at 9.555 *ps* where specific imaginary frequency of 2094.3*i* cm^{-1} was obtained. It corresponds to vibrations of both H1 and H2 protons separated by the distance of 5.407 Å (respective CRYSTAL output file 9_555_ps.out is supplied as SEM including vibrational vectors for all 51 modes, where the H1 and H2 amplitudes are given just after the title "Normal Modes Normalized To Classical Amplitudes (In Bohr)". The second component of these coupling H1-H2 modes seems to be real with the frequency of 2224.07 cm^{-1}) This specific coordinate with imaginary frequency is absent in other time moments so that it is impossible to compare the different systems along the AIMD trajectory with this moment 9.555 ps. It was not described in the CRYSTAL manual how the entropy is calculated if a frequency is imaginary. It looks like this mode is deleted from the consideration automatically. But if the deletion of the single small imaginary frequencies (at the Rea(2), 2.495, 4.480, and 6.095 ps) did not really influence on the total entropy, the deletion of this large 2094.3*i* frequency essentially changed it. We have to delete it to be coherent without a possibility to remove similar mode at other *i*-points as it was done at the PBE-D3. Then the RMS deviation relative to the TS average of 1.284 eV/cell takes 0.061 eV/cell along the 8 points in Table S2. (This RMS deviation grows up to 0.075 eV/cell while including the «bad» 9^{th} point at 9.555 ps.) The RMS boundary for ΔG is slightly larger than maximal (in absolute values) deviations of -0.027 and 0.042 eV/cell at the PBE-D3/PAW level. These evaluations of the entropy terms showed the reasonability of the enthalpy consideration when kinetic modelling (and kinetic constants based on the free energy) could hardly give a new interpretation.

Part S2. The motivation and place of the current study

This work is a part of the 10-year study of carbonates in zeolites. They started by 2012 from the justification of the carbonate's influence on K^+ cations and its displacement from 8R using the "static" calculation of enthalpy (*via* the observation of a series of deep local minimum far outside of the 8R plane) in NaKA zeolite[12]. Later it was confirmed at the level of AIMD calculation for the same NaKA system[13]. In between these two studies[12,13] the relation between carbonate's geometry and band splitting of in IR spectra[69], the changes of elastic moduli of the zeolites due to the carbonate's formation[49,50], distortions of the 8R windows upon alkali cation's influence in MeRHO zeolites[53], alternative routes of carbonate's formation[69], influence of particularly high carbonate concentration in CsY (relative other alkali Y forms) on the heat of CO_2 adsorption[17], drift of the cations for shielding the formation of carbonate's anions[32], activation barriers for reaction (1) in MeX[32,33] *etc.* were analyzed.

An attempt to visualize the passage of CO_2 through 8R window at the displaced $K^+ \ldots CO_3^{2-}$ after the work[13] required a high CO_2 concentration in one of two α-cages joined/separated by the 8R window with K^+ cation in the NaKA zeolite. The attempt did not show the CO_2 passage within too short AIMD time (~20 ps) but at the presence of 7 CO_2 and one CO_3^{2-} (high CO_2 loading) *per* one α-cage it was found that the formation of dicarbonate $C_2O_5^{2-}$ is quite easily after 1 ps of AIMD run being irreversible (Fig. 1d, Part 3.1.1). In order to verify the same possibility of dicarbonate's formation at low CO_2 loading a confirmation was successfully obtained at the presence of only one CO_2 and one CO_3^{2-} at the next step of our AIMD studies (Part 3.1.2). In the last case the $C_2O_5^{2-}$ formation was however reversible (Fig. 4a). The cNEB algorithm for calculating moderate activation for different alkali cations also have been applied at low CO_2 loading (Part 3.2) because additional CO_2 molecules can elongate the reaction coordinate (due to CO_2 parallel displacement in the course of the reaction) thus requiring very long computations. Additional CO_2 molecules can result in more complex influence on the dicarbonate spectra so that they were omitted while calculating IR frequencies and intensities (low CO_2 loading in Part 3.3). "Static" optimization of the system of 6 CO_2 and one $C_2O_5^{2-}$ (high

CO_2 loading) using VASP allowed to obtain a local minimum for slightly less stable system of 5 CO_2 and one $C_3O_7^{2-}$ tricarbonate anion (Part 3.4, Fig. 5b). In all cases non-hydrated cations in 8R window were involved into reaction (3) or the formation of tricarbonate that is totally justified by minor concentration of water which remains after the dehydration of the zeolites according to the experimental conditions[16, 28-31] at which IR spectra were studied.

To solidify our conclusions about a possibility of the reaction (3) the vibrational entropy for low loading as the most important part of the entropy in some points along the AIMD trajectory (Part S1). The comparison of the vibrational entropy was calculated for high loading is hindered owing to the numerous imaginary frequencies for CO_2 positions because the CO_2 are not in the local minimum of the energy. Such comparison between different points along the AIMD trajectory analysis becomes very complex due to different imaginary frequencies of different CO_2 molecules.

In our study only one CO_3^{2-} was considered after reaction (1) irrespective of the CO_2 loading. This restriction is based on the experimental estimations in NaCaY[14] and NaX.[15] At high Ca content (> 60%) two CO_3^{2-} species per FAU unit cell (one CO_3^{2-} per two large cavities) were confirmed from IR data.[14] The pore volume in NaCaY is larger than that in NaX but the cation concentration is higher in NaX. These opposite conditions make difficult to select either NaCaY, or NaX for the best CO_3^{2-} stabilization. For the latter, the "dead" volume blocked by chemisorbed CO_2 was estimated experimentally (8%) to be lower than in $Na_{12}A$ (18 %).[15] Earlier a decrease of elastic moduli was tested for the coverage of one CO_3^{2-} *per* each large cavity in NaX (Si/Al = 1). The Young moduli has been reduced by around 5 %, which is a large value compared to the reduction caused by direct dealumination at the same computational PBE/PAW level.[48,49] So we believe that the presence of two CO_3^{2-} per one large α-cavity of NaMeA is less likely because the α-cages of NaMeA are smaller than that of NaX, for which one observed a critical change of the NaX elastic properties even at lower CO_3^{2-}concentration.

Table S1. The contribution to Gibbs energy (eV/cell) from vibrational entropy variations for the optimized initial (Rea(2)) and final (Pro(2)) geometries along the reaction (2) and selected points of the AIMD modelling of the reaction (3) (time at these points is shown in *ps* relative to the scale of the Fig. 4a, see respective arrows) with one CO_2 molecules and one CO_3^{2-} anion per UC calculated at the PBE-D3/PAW level.

Points	$T\Delta S_{vib}$
Rea(2)[a)]	-0.025
Pro(2)[b)]	0.000
2.495	0.030
4.480	0.042
6.065	0.030
6.140	-0.011
6.166	0.000
9.555	-0.027

[a)] Rea(2) is related to the reagents in Fig. 3; [b)] Pro(2) corresponds to 0 ps in Fig. 4a.

Table S2. The TS contribution (eV/cell, at 298.15K) to Gibbs energy including vibrational entropy (for 17 vibrating atoms), numbers (N) and imaginary frequencies ω (cm^{-1}) for the optimized initial (Rea(2)) and final (Pro(2)) geometries along the reaction (2) and selected points of the AIMD modelling of the reaction (3) (time at these points is shown in ps relative to the scale of the Fig. 4a, see respective arrows) with one CO2 molecules and one CO_3^{2-} anion per UC calculated at the B3LYP level.

Points	TS	N	$-i\omega$
Rea(2)[a)]	1.280	2	48.4, 16.9
Pro(2)[b)]	1.346	0	-
2.495	1.213	1	5.5
3.065	1.279	0	-
4.480	1.224	1	7.9
6.065	1.219	0	-
6.095	1.215	1	114.1
6.140	1.299	0	-
6.166	1.196	0	-
9.555[c)]	1.140	1	2094.3

[a)] Rea(2) is related to the reagents in Fig. 3; [b)] Pro(2) corresponds to 0 ps in Fig. 4a; [c)] respective CRYSTAL output file 9_555.out is supplied as SEM (TS values are shown at the end, search of the entropies under the title “Thermodynamic Functions With Vibrational Contributions”)

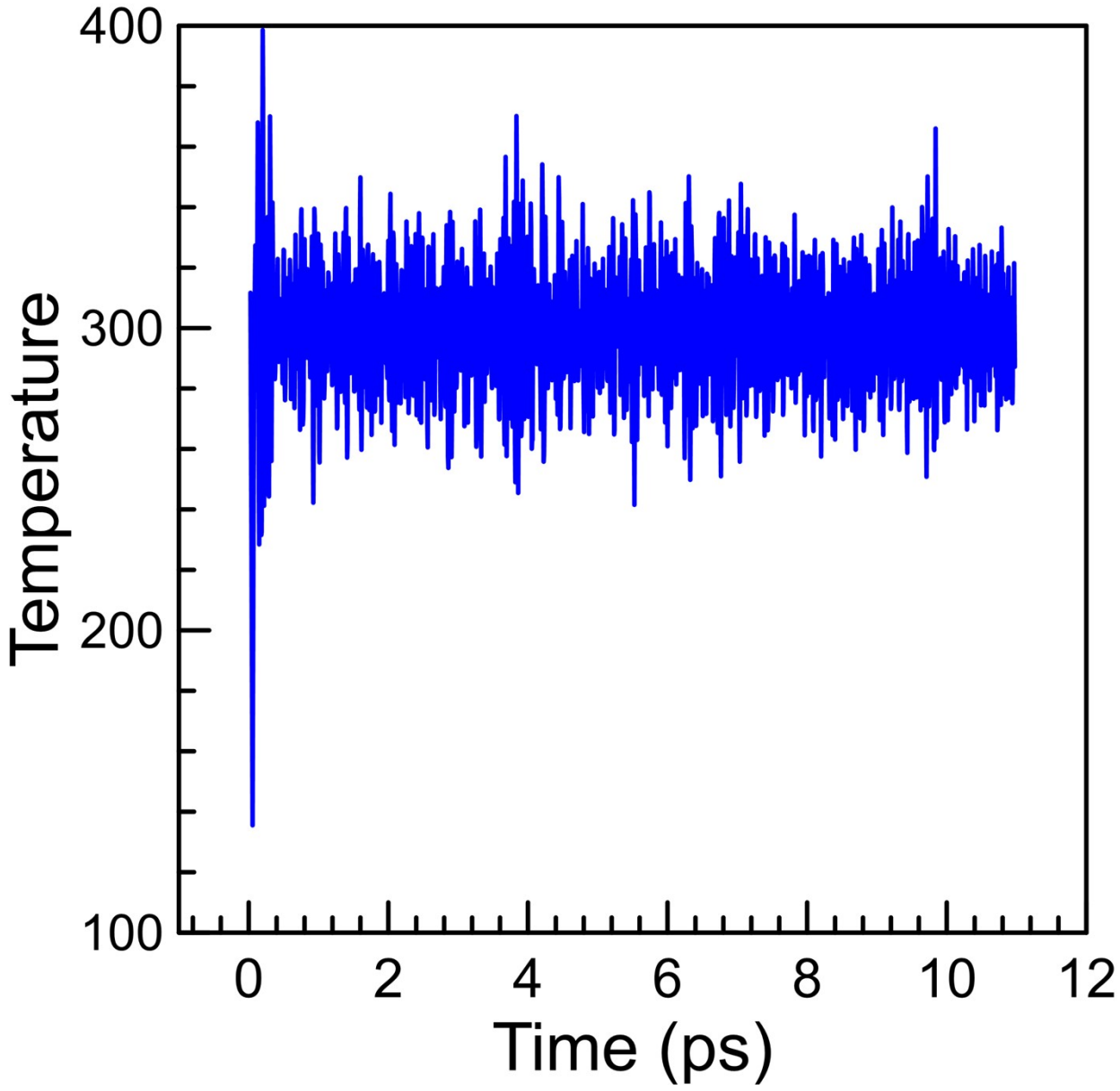

Fig. S1. Thermal equilibration (K) for the reaction (3) with one CO_2 and one CO_3^{2-} species (low loading) at the PBE-D3 level.

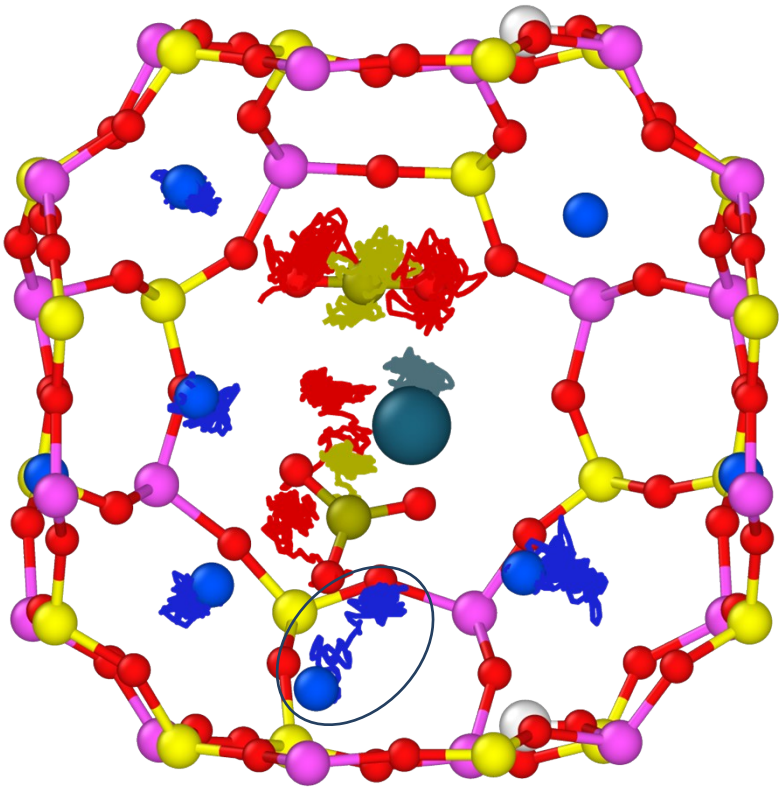

Fig. S2. Trajectories of Na and K cations, C and O atoms are shown by the same colors as the atoms for the reaction (3) between one CO_2 and one CO_3^{2-} species (low loading) in the course of AIMD run at the PBE-D3 level (initial positions of the atoms at $t = 0$ *ps* are given). The ellipse shows the NaII atom which leaves the 8R window approaching the carbonate. All atoms are allowed to move but the trajectories are shown only for a part of the atoms which participates in the reaction (A trajectory of one O atom of the CO_3^{2-} group is not shown due to a complexity with different boundaries used by the MOLDRAW code at different steps of the AIMD presentation.). The atomic colors are given in gray, olive, red, blue, magenta, yellow, and dark blue for H, C, O, Na, Al, Si, and K, respectively.